3-2-8 Observations of Plasma Bubbles by HF-TEP and GPS Scintillation

SAITO Susumu, MARUYAMA Takashi, ISHII Mamoru, and KUBOTA Minoru

GPS scintillations were observed at Hainan, China (19.5˚N, 109.1˚N) and Phu Thuy, Vietnam (21.0˚N, 106.0˚E) to compare with the transequatorial propagation of HF radio waves (HF-TEP) observed at Oarai, Japan (36.3˚N, 140.6˚E). The results show that the GPS scintillation occurrences at Hainan at nighttime were well coincided with the off-great circle propagation (OGCP) occurrence in HF-TEP of Radio Australia observed at Oarai. This confirms that the OGCP at nighttime corresponds to the plasma bubble occurrence. At Hainan and Phu Thuy, respectively, three GPS scintillation receivers were installed with about 100 m separation to measure the drift velocity of small-scale ionospheric plasma irregularities associated with plasma bubbles. On the other hand, the drift velocity of large-scale bottomside ionospheric structures associated with plasma bubble can be estimated by the change in arrival angles of HF-TEP. Measured velocities by these two methods were similar to each other. Our results show that the HF-TEP measurements are effective in monitoring plasma bubbles in wide area and forecast their arrival.

Keywords
Plasma bubble, Ionospheric irregularity, HF-TEP, GPS scintillation, Monitoring and prediction of plasma bubble propagation

1 Introduction

Observing the HF trans-equatorial propagation (HF-TEP) of HF radio waves has long been used as a means of observing large-scale ionospheric irregularities in the equatorial region. Since radio waves travel straight, short waves often arrive in the great-circle direction relative to the radio wave source, but may sometimes come from a direction deviated from the great-circle direction. Röttger[1] performed an experiment on sending and receiving short waves between Lindau, Germany, and Tsumeb, Namibia, thereby demonstrating the existence of a large-scale corrugated structure that travels eastward at nighttime, and which is accompanied by equatorial spread F. Maruyama and Kawamura[2] utilized the latest HF direction finding system to observe HF-TEP by using broadcast waves from Australia, and discovered a phenomenon whereby the direction of arrival emerges in the west away from the great circle direction and then gradually changes course southward. They estimated that this off-great circle propagation (OGCP) was due to the large-scale structure of an eastward traveling ionospheric substructure near the equator, and determined its typical velocity to be about 200 m s^{-1}. Moreover, based on the velocity characteristics and seasonal dependency of OGCP occurrence (including local maximums around the spring equinox and autumn equinox), and other factors, they concluded that the trans-equatorial OGCP of HF radio waves at nighttime is due to plasma bubbles, and that observing HF-TEP affords a means of monitoring the generation of plasma bubbles in a wide area. However, their observations offered no direct evidence linking the OGCP of HF radio waves at nighttime to plasma bubbles.

Plasma bubbles contain plasma irregularities with various wavelengths. When a radio wave in the VHF or UHF band passes through a plasma bubble, Fresnel diffraction causes the amplitude and phase to change—observed on the ground as scintillation. Scintillation can disrupt satellite communications and positioning, but has also been used to detect ionospheric irregularities. Scintillation caused by Fresnel diffraction is intensely generated when a radio wave of certain wavelength λ goes through a plasma irregularity having a horizontal scale of $\sqrt{2\lambda h}$ existing at altitude h. In recent years, measurement of the scintillation on GPS satellites has not only helped to detect plasma bubbles but also to measure the drift velocity of irregularities with plasma bubbles by using multiple receivers installed spatially separated (the spaced-receiver method)[3]-[7]. The large electron density gradient and plasma irregularities stemming from plasma bubbles pose a hazard to the more advanced use of satellite positioning and satellite communications, which makes it very important to monitor the generation and movement of plasma bubbles in a wider area.

In the spaced-receiver method, when plasma irregularities exist at an altitude between 250 and 400 km with the L1 frequency (1.57542 MHz) of GPS, $\sqrt{2\lambda h}$ becomes 300 to 400 m and will be used in measuring the drift velocities of those irregularities on a horizontal scale of this magnitude as contained in plasma bubbles. Here, it is not that the drift velocity of plasma bubbles themselves is measured as the region of electron density depletion. In fact, to clarify the relation between the drift velocity of plasma bubbles and that of small irregularities, simultaneous observations[8] were conducted by taking optical images of plasma bubbles from an IMAGE satellite and measuring plasma drift velocity by using the ROCSAT-1, thereby demonstrating a significant difference between the two. Assuming that this result is correct, measuring the velocity of small irregularities stemming from plasma bubbles that cause scintillation will not necessarily result in the same velocity of plasma bubbles. This will pose a major problem when predicting the movement of plasma bubbles by using the velocity derived from observing scintillations. It is consequently very important to measure the velocity of irregularities on various spatial scales stemming from plasma bubbles, and determine the relation between the spatial scale of irregularities and their drift velocity.

Based on the background of studies described above, this study aims to determine the large-scale structure of the bottom side ionosphere that causes OGCP as seen in HF-TEP observations (whether consisting of plasma bubbles or something else), and observe changes in the arrival angle of OGCP and GPS scintillation by using the spaced-receiver method to determine the relation between the spatial scale and drift velocity of irregularities.

This report is based on the work by Saito et al[6]. as published by the Journal of Geophysical Research in 2008.

2 Observation and Analysis

This study observed HF-TEP in Oarai, Japan (36.3°N, 140.6°E), while conducting observations by using GPS scintillation and the spaced-receiver method at Hainan, China (19.5°N, 109.5°N, magnetic latitude +13.9°) and Phy Thuy, Vietnam (21.0°N, 106.0°E, magnetic latitude +15.7°).

2.1 HF-TEP

As the source of radio waves for HF-TEP, broadcast waves emitted from Radio Australia in Shepparton, Australia (36.02°S, 145.3°E) were used. These waves were received by using the HF direction finding system (Oarai direction finder: ODF) installed in Oarai, Japan. Shepparton and Oarai are in almost the same geographical meridian plane and a distance of about 8,000 km separates both locations (Fig. 1). At about 140°E longitude, the magnetic equator is located at about 8°N latitude, so that the relation between both points concerns geographical south and north conjugate points rather than magnetic conjugate points. The direction of Shepparton as viewed

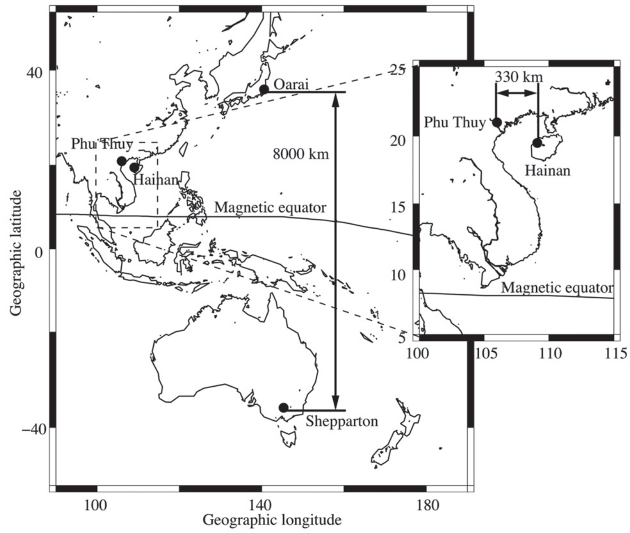

Fig.1 *Composition chart of the observation. It shows Radio Australia's point of transmission, the direction finding system in Oarai, observation points of GPS scintillation, and location of the magnetic equator* [9].

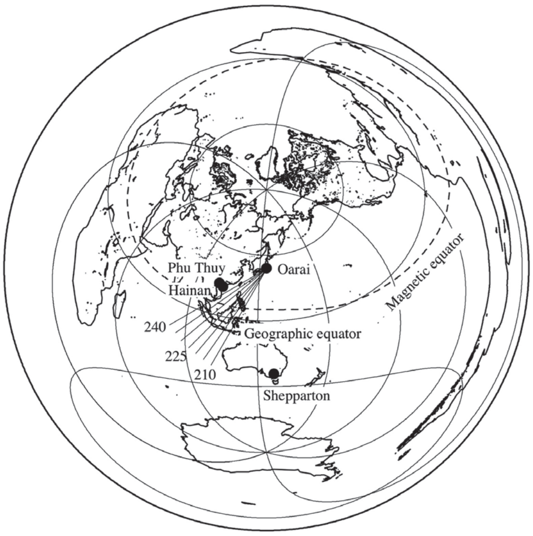

Fig.2 *Relation between the azimuth angle on one hand and each observation point and the magnetic equator on the other as observed in Oarai per azimuthal equidistant projection. The radial lines centered on Oarai show the azimuth angle from Oarai (positive clockwise assuming that due north is 0°) in increments of 5° from 210° to 240°* [9].

from the reception point at Oarai is 175.7° clockwise from due north. The ODF consists of antenna arrays composed of seven orthogonal loop antennas arranged on a circle with a diameter of 60 m, and the MUSIC method is employed to determine arrival directions (i.e., azimuth and elevation angles) of up to three waves at the same time with an angular resolution of 1° and time resolution of 0.5 second. Radio Australia provides broadcasts around the clock, but its transmission frequency changes depending on the season and local time. The observations in this project were made by scanning all frequencies that may be used in broadcasts by Radio Australia. Reception frequency scanning was done using the following procedure: Reception at that frequency, measurement of the arrival directions for 8 seconds when the signals are found, and then shifting to the next frequency.

In assuming that the OGCP of Radio Australia's broadcast waves observed at Oarai is due to a single mirror reflection attributed to the ionospheric plasma density gradient stemming from plasma bubbles, since Oarai and Shepparton are at the geographical south and north conjugate points, the reflection point can then be assumed near the geographical equator. Plasma bubbles have such a long structure in the north-south direction[10][11] that when one plasma bubble is observed at a certain point, the same plasma bubble can be assumed to exist near the geographical equator at the same longitude as that point. The geographical equator at the longitude of Hainan with its GPS scintillation observation equipment is at a azimuth angle of 226° as viewed from Oarai (Fig. 2); therefore, in assuming that the OGCP of Radio Australia's broadcast waves stems from plasma bubbles which have reached the latitude within the field of view of Hainan's observation equipment, we can also expect that scintillation can be observed at the same time over Hainan. The OGCP of Radio Australia's broadcast waves is not necessarily reflected only near the geographical equator. And since the substructure of plasma bubbles may be bent relative to the longitudinal line, the azimuth angle of OGCP will probably have some dispersions with regard to 226°.

2.2 GPS scintillation

Hainan and Phy Thuy—where the GPS scintillation observation equipments utilizing the spaced-receiver method are installed—are located about 330 km apart east and west (Fig. 1). Table 1 lists the specifications for the GPS scintillation equipment installed at Hainan and Phu Thuy. Both points are equipped with three GPS receivers each. Two Ashtech G12 receivers and one Ashtech BR2G receiver are installed at Hainan where the carrier-to-noise ratio (CNR) was recorded at 20 Hz. At Phu Thuy, three JAVAD LGG-100 receivers were used to record CNR at 100 Hz. At both points, the three receivers were installed at distances of 90 to 100 m apart as shown in Fig. 3. The CNR recorded was used to derive the S_4 scintillation index; the maximum value of the cross-correlation function between receivers, and the time lag that gives maximum correlation were derived at increments of 60 seconds. The S_4 index is a normalized standard deviation of the variations and, assuming that CNR is s, it can be expressed by the following equation:

$$S_4 = \sqrt{\frac{\langle s^2 \rangle - \langle s \rangle^2}{\langle s \rangle^2}} \tag{1}$$

Table 1 *Specifications of the observation systems for GSP scintillation*

Location	Hainan	Phu Thuy
Geographic latitude	19.5ºN	21.0ºN
Geographic longitude	109.1º	106.0º
Magnetic latitude	+13.9º	+15.7º
Receiver model	Ashtech G12/BR2G	JAVAD LGG100
Frequency	L1 (1.57542 GHz)	L1 (1.57542 GHz)
Data acquisition rate	20 Hz	100 Hz

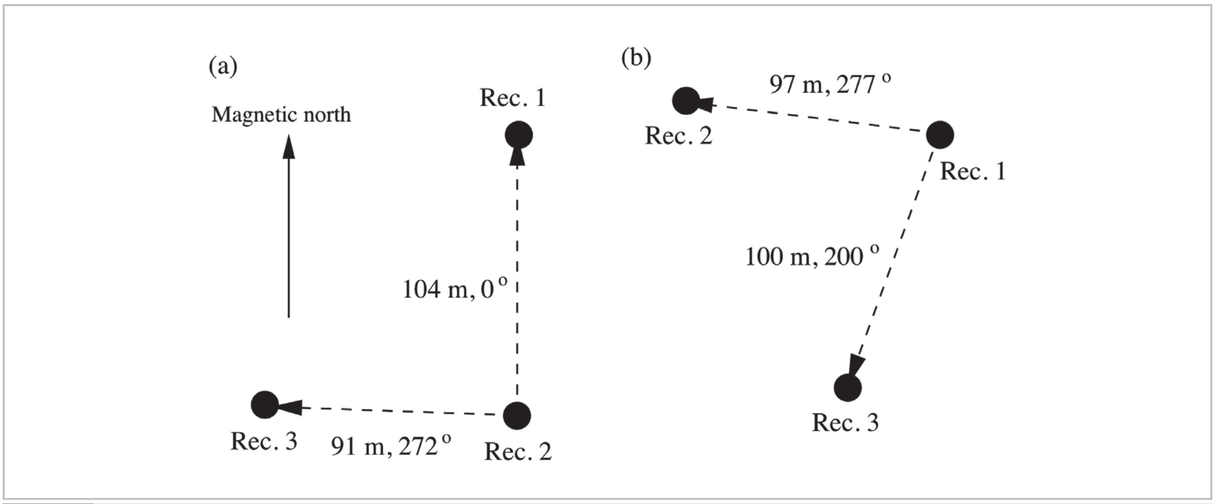

Fig.3 (a) Layout of the GPS receiver antennas in Hainan, China; (b) Layout in Phu Thuy, Vietnam The angles in the figures represent the relative locations between receiver antennas as measured clockwise from magnetic north [9].

Assuming a plane wave, the time lag obtained between receivers allows the drift velocity (and direction) of the scintillation pattern to be derived. This method is known to cause errors in velocity when the scintillation pattern changes in time[12], but CNR changes due to irregularities stemming from the plasma bubbles normally have a very high correlation at distances of about 100 m (meaning that, assuming movement at about 100 m s-1, the scintillation pattern hardly changes at about one second). This error can therefore be ignored[5]. The drift velocity of irregularities in the ionosphere can be derived from that of the scintillation pattern on the ground, and from GPS satellite location and velocity. In this study, the drift velocities of irregularities were derived by using the method of Ledvina et al.[6]. The scintillation pattern on the ground is determined by the mutual relationship of the receiver, plasma irregularities, and GPS satellite location and velocity. The irregularities are believed to be elongated along the magnetic lines, so that the shape and movement of the scintillation pattern generated on the ground can be understood as being analogous with the shades of irregularities generated on the ground illuminated by light from the satellites. The reader should understand that the aboveground movement of shades is determined by synthesis of the movement of irregularities that constitute shades in the direction perpendicular to the magnetic field lines and with satellite movement serving as a light source. The irregularities can be considered to be elongated very long along the magnetic field line, so that the scintillation pattern on the ground can be considered to constitute a plane wave. At that time, the only observable quantity is the component perpendicular to the wave front, and any existing component parallel to the wave front cannot be observed. In other words, attention must be paid to the fact that velocity measured by movement of the scintillation pattern on the ground is not a two-dimensional vector but a scalar. Moreover, plasma bubbles develop in the direction of altitude, while scintillation intensity is proportional with the absolute amplitude of the irregularities, so that the effect is considered most intense near the peak of the ionospheric F region. From this, we can assume that irregularities exist at a certain range of altitude. This study assumed that irregularities exist at an altitude of 300 km. The point at which the line of sight between satellite and receiver crosses this altitude is called the ionospheric piece point (IPP). Here, in assuming z_{sat} to denote satellite altitude, z_{ion}

the ionospheric altitude (= 300 km), v_{ion} the velocity of irregularities in the stationary orthogonal coordinate system (a left-hand system with y in magnetic north and z in vertically up), and v_{sat} the satellite velocity, the eastward velocity of the scintillation pattern on the ground can be expressed as:

$$v_{scintx} = \frac{z_{sat}}{z_{sat} - z_{ion}} \left\{ v_{ionx} + (q_y/q_x) v_{iony} + (q_z/q_x) v_{ionz} - \frac{z_{ion}}{z_{sat}} \left[v_{satx} + (q_y/q_x) v_{saty} + (q_z/q_x) v_{satz} \right] \right\} \quad (2)$$

Let the velocity of irregularities in the coordinate system orthogonal with the magnetic field line at IPP (a left-hand system with x eastward and z upward and perpendicular to the magnetic field line) be v_{ipp}, which can be expressed using a 3×3 transform matrix **R** as:

$$\mathbf{v}_{ipp} = \mathbf{R}\mathbf{v}_{ion} \quad (3)$$

The matrix R is determined by the receiver's location, direction of the magnetic field line, and IPP location (satellite location). For details, refer to Equations 4 to 8 in Ledvina et al.[6]. The eastward velocity of irregularities at IPP and the velocity upward and perpendicular to the magnetic field line can be expressed by using the [i,j] component R_{ij} of the matrix **R** as follows:

$$\begin{bmatrix} v_{ippx} \\ v_{ippz} \end{bmatrix} = \begin{bmatrix} R_{11} - \frac{R_{21}R_{12}}{R_{22}} & R_{13} - \frac{R_{21}R_{32}}{R_{22}} \\ R_{13} - \frac{R_{23}R_{12}}{R_{22}} & R_{33} - \frac{R_{23}R_{32}}{R_{22}} \end{bmatrix} \bullet \begin{bmatrix} v_{ionx} \\ v_{ionz} \end{bmatrix} \quad (4)$$

Here, defining matrix **S** as follows:

$$\mathbf{S} = \begin{bmatrix} R_{11} - \frac{R_{21}R_{12}}{R_{22}} & R_{13} - \frac{R_{21}R_{32}}{R_{22}} \\ R_{13} - \frac{R_{23}R_{12}}{R_{22}} & R_{33} - \frac{R_{23}R_{32}}{R_{22}} \end{bmatrix}^{-1} \quad (5)$$

where, $[\,]^{-1}$ denotes matrix inversion, Equation (1) can be rewritten as follows:

$$v_{scintx} = \frac{z_{sat}}{z_{sat} - z_{ion}} \Bigg\{ \left[\left(1 - \frac{q_y}{q_x}\frac{R_{21}}{R_{22}}\right) S_{11} + \left(\frac{q_z}{q_x} - \frac{q_y}{q_x}\frac{R_{23}}{R_{22}}\right) S_{21} \right] v_{ippx} + \left[\left(1 - \frac{q_y}{q_x}\frac{R_{21}}{R_{22}}\right) S_{12} + \left(\frac{q_z}{q_x} - \frac{q_y}{q_x}\frac{R_{23}}{R_{22}}\right) S_{22} \right] v_{ippz} - \frac{z_{ion}}{z_{sat}} \left[v_{satx} + \frac{q_y}{q_x} v_{saty} + \frac{q_z}{q_x} v_{satz} \right] \Bigg\} \quad (6)$$

In Equation (6), v_{ippx} and v_{ippz} are the unknown quantities. Both cannot be determined at the same time. In this analysis, we therefore assume v_{ippz} as 0. This assumption holds when the contribution of v_{ippz} is sufficiently smaller than that of v_{ippx}, but is inappropriate in case the velocity of irregularities has a upward component perpendicular to the magnetic field line that cannot be ignored. However, after the plasma bubbles have been developed, the upward component perpendicular to the magnetic field line is generally small. Fejer et al.[13]. reported that the upward velocity perpendicular to the magnetic field line following the prereversal enhancement period after sunset is about one-fifth of the east-west component. From this we decided, for this study, to only analyze cases where the coefficient of v_{ippz} is not more than half the coefficient of v_{ippx}, so that the contribution of v_{ippz} can be suppressed to no more than one-tenth of the contribution of v_{ippx}.

3 Results

Figure 4 shows the arrival azimuth angle (positive clockwise with due north set to 0°) of Radio Australia as observed by ODF on March 29, 2007. The data near the azimuth angle of 176° stem from great-circle propagation, and this is called the "main trace" [2]. In contrast, the group of data seen to the west of the main trace between 12:00 and 19:00 UT due to OGCP is called a "satellite trace". The data near 260° at 10:30 to 12:00 UT, near 260° at 14:00 to 16:00 UT, or near 260° at 17:00 to

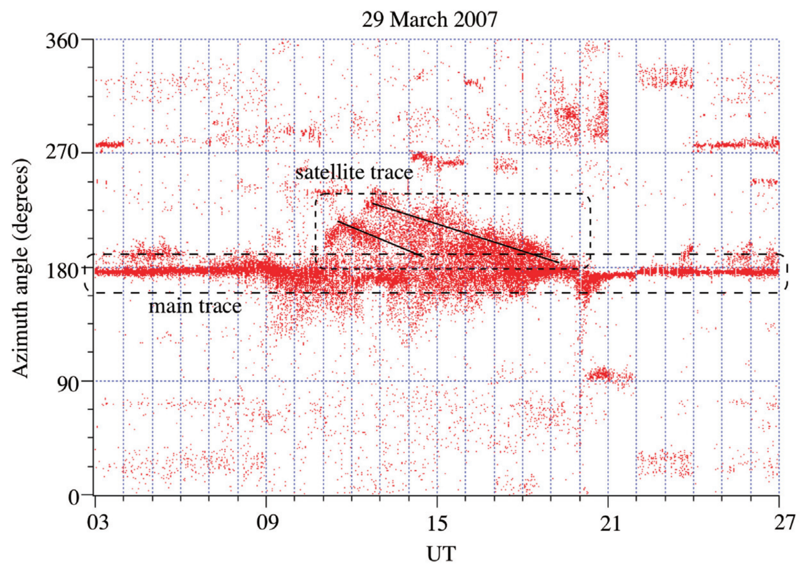

Fig.4 *Arrival angle of broadcast waves from Radio Australia observed in Oarai on March 29, 2007*
The arrival angle was taken with geographical north at 0˚ and positive clockwise [9].

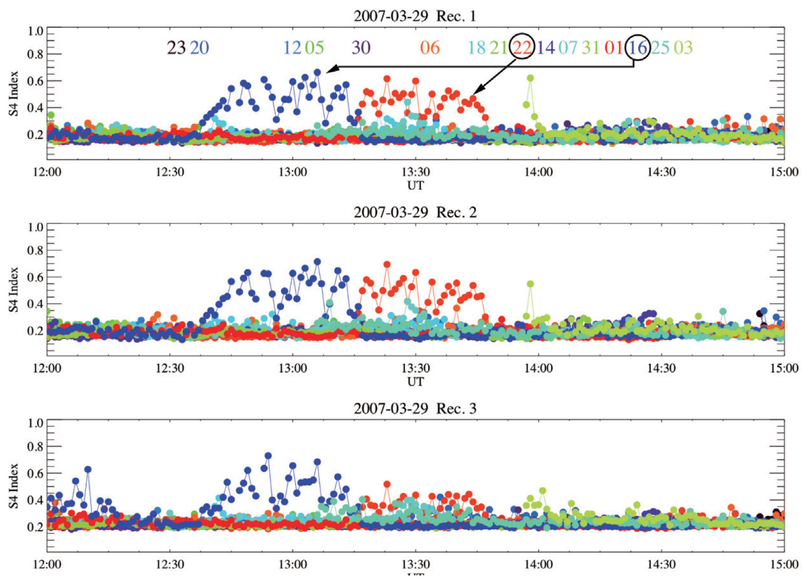

Fig.5 *S_4 indices of GPS scintillation observed at Hainan on March 29, 2007*
The S_4 indexes of different satellites are color-coded to match the color of the satellite number (PRN) shown in the topmost figure [9].

18:00 UT are known to be due to sources of radio waves other than Radio Australia. The arrival direction of data belonging to a satellite trace changes southward with time, and the reflection point is considered to have moved eastward. Maruyama and Kawamura [2] thought that this might correspond to the eastward movement of the large-scale structure of the bottom side ionosphere stemming from plasma bubbles. By using the method employed by Maruyama and Kawamura [2] and based on temporal changes in the arrival angle, we estimated the velocity of the reflection point as being 93 m s^{-1} eastward. As is evident from Fig. 4, however, the satellite trace is obscure and the slope as a source in estimating velocity has a certain degree of range. Even with the slope being clearly determined, this method entails error of 7 to 8 m s^{-1}; therefore, note that the estimation error in actual velocity will be even larger.

On the same day the satellite trace was observed in Oarai, Hainan observed intense GPS signal scintillation. Figure 5 shows the S_4 index of GPS L1 signal intensity observed at Hainan on March 29, 2007. In response to the GPS L1 signals of PRN 16 and 22, a large S_4 index was observed between 12:40 and 13:15 UT and between 13:15 and 13:45 UT, respectively. At that time, no scintillation was observed at Phu Thuy. Figure 6 shows the maximum correlation values between the three

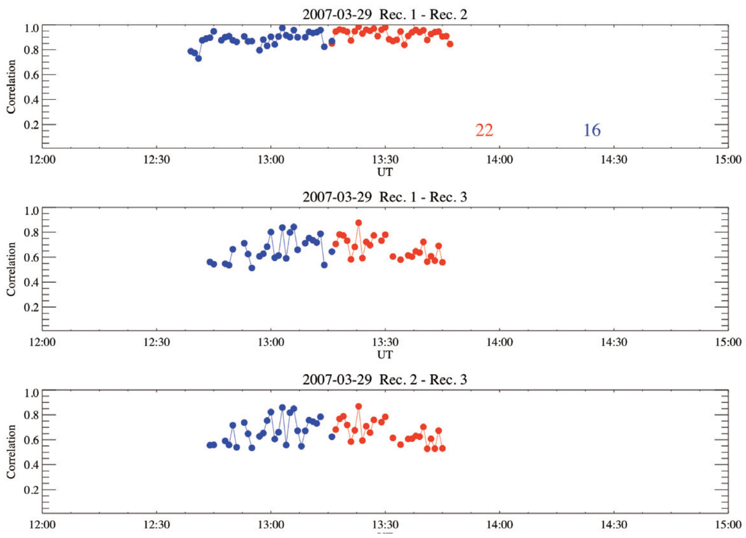

Fig.6 Correlation coefficients of changes in received intensity between antennas observed at Hainan on March 29, 2007
The figure only shows cases with S_4 indexes of 0.3 or more. The blue line shows data regarding the PTN 16 satellite; the red line shows data regarding the PRN 22 satellite [9].

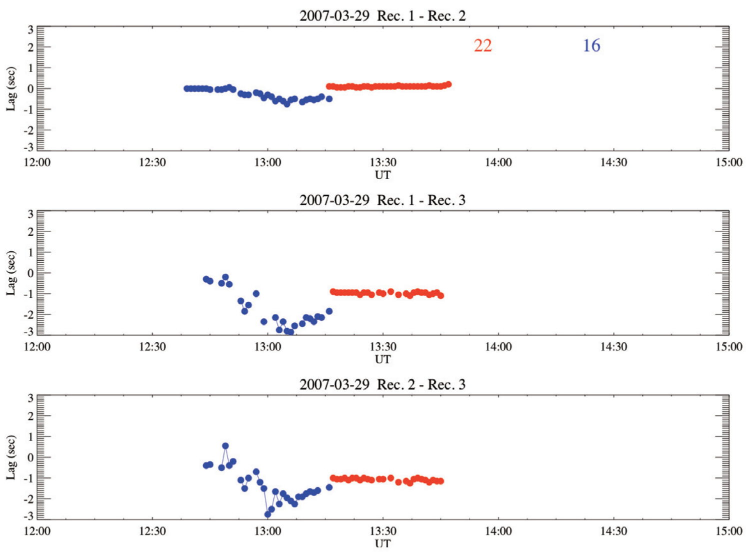

Fig.7 Time lags of changes in received intensity between antennas observed at Hainan on March 29, 2007
The figure only shows cases with S_4 indexes of 0.3 or more. The blue line shows data regarding the PRN 16 satellite; the red line shows data regarding the PRN 22 satellite [9].

receivers regarding the temporal variation of CNR of the PRN 16 and 22 satellites in Hainan; Figure 7 shows the time lags corresponding to the maximum correlation values shown in Fig. 6. In these figures, data with an S_4 index of 0.3 or more are plotted. There may seem to be no continuity between PTN 16 and 22 data. However, as discussed above, movement of the scintillation pattern on the ground is determined by the mutual relationship between the receiver, plasma irregularities, and satellite location and velocity; therefore, scintillations due to irregularities stemming from the same plasma bubble can be reasonably expected to cause discontinuity in temporal differences between receivers located between different satellites. These time lags were used to measure drift velocity of the scintillation pattern on the ground and estimate the drift velocities of plasma irregularities by using Equation (6). Figure 8 shows the results. Here, the data of PRN 16 were not used to estimate velocities due to the conditions for estimating velocities obtained from Equation (6) (where the coefficient of v_{ippz} is not more than half of the coefficient of v_{ippx}). From Fig. 8, the drift velocity of plasma irregularities estimated at that time was about 130 m s^{-1} eastward. It can be seen that the drift velocity of these plasma irregularities estimated based on GPS scintillation is in reasonable agreement with the drift velocity of the large-scale structure of the bottom side ionosphere estimated based on HF-TEP.

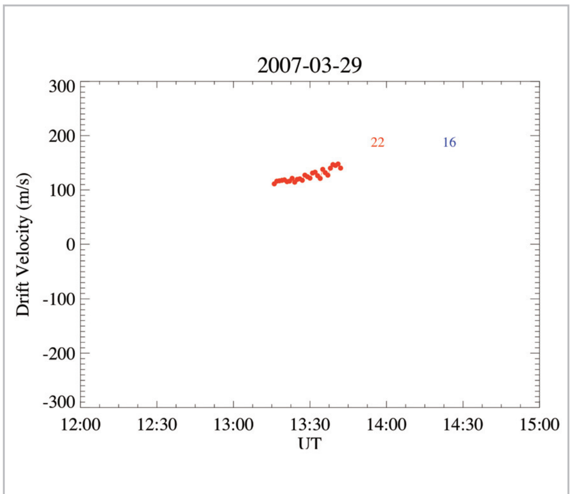

Fig.8 *Drift velocity of irregularities as derived by using the correlation in temporal variation of CNR between antennas observed at Hainan on March 29, 2007*
The figure only shows cases where the S_4 index was 0.3 or more and the condition regarding Equation (6) was satisfied. The blue line shows data regarding the PRN 16 satellite; the red line shows data regarding the PRN 22 satellite [9].

During the period from March to October 2007, OGCP was observed by ODF near 226° on March 26, 29 and 31, September 18 and 22, and October 22 (six nights). GPS scintillation presumably stemming from plasma bubbles over Hainan was observed on March 26, 29 and 31, on April 1 and 15, September 18, and October 22, 2007. The observation system in Phu Thuy was regrettably in poor condition, and therefore a significant conclusion could not be reached except on March 29, 2007. Table 2 summarizes the dates of OGCP occurrence as observed by ODF and the dates of GPS scintillation over Hainan and Phu Thuy. Table 3 lists the periods of OGCP occurrence near the azimuth angle of 226° at ODF and the periods of GPS scintillation over Hainan. However, since the poor condition of ODF resulted in a lack of HF-TEP data on April 15, 2007, the data were excluded from Table 3. From these results, it can be seen that OGCP near the azimuth angle of 226° at ODF and GPS scintillation over Hainan agree very well. Moreover, the OGCP generally occurred earlier at ODF and ended later than GPS scintillation at Hainan. This suggests that the large-scale structure of the bottom side ionosphere that presumably causes OGCP in HF-TEP is generated before plasma bubbles form and lasts longer than plasma irregularities with a scale size of a few hundred meters that cause GPS scintillation, and that observations by using GPS scintillation are conducted at the point where the line of sight between satellite receivers crosses the ionosphere, while HF-TEP is a two-dimensional observation that covers a wider range than the GPS receiver at a time.

Table 2 *Dates of OGCP of HF-TEP and GPS scintillation occurrence*

Date	OGCP Oarai (near the azimuth angle of 226°)	GPS scintillation Hainan	 Phu Thuy
March 26, 2007	O	O	ND
March 29, 2007	O	O	NO
March 31, 2007	O	O	ND
April 15, 2007	ND	O	ND
September 18, 2007	F	O	ND
October 22, 2007	O	O	ND

Note that O, NO and ND denote occurrence, non-occurrence, and lack of measurement, respectively. On September 18, 2007, faint OGCP was observed, thereby being expressed as F.

Table 3 *Times (UT) of OGCP occurrence at Oarai and GPS scintillation at Hainan*

Date	Oarai (near the azimuth angle of 226°)	GPS scintillation (Hainan)
March 26, 2007	11:50-15:30	12:40-15:00
March 29, 2007	11:30-15:00	12:40-13:45
March 31, 2007	11:30-17:00	12:20-14:00
September 18, 2007	14:45-17:00	14:30-16:00
October 22, 2007	11:00-14:00	13:30-13:55

4 Discussion

Figure 9 (a) shows the GPS satellite's trajectory of IPP at an altitude of 300 km seen from Hainan. The red lines indicate the interval where scintillation was observed. Figure 9 (b) shows the GPS satellite's trajectory of IPP at an altitude of 300 km seen from Phu Thuy; the red lines indicate the location where scintillation was observed at Hainan, similarly to Fig. 9 (a). From this, it is evident that the trajectory of IPP over Phu Thuy deviates from the red lines. The trajectory of IPP for the PRN 18 satellite seen from Phu Thuy appears to be near the location where scintillation of the PRN 22 satellite signal was observed at Hainan. However, the time of day when the PRN 18 satellite's trajectory over Phu Thuy intersected with the location indicated by the red lines differs from the time of day when scintillation was observed by the PRN 22 satellite signal, and the PRN 18 satellite passed over Phu Thuy toward the southeast without encountering the plasma bubble. From these findings, one can understand why no scintillation was observed at Phu Thuy even though it was observed at Hainan. Moreover, the observation of plasma bubbles by using GPS scintillation is essentially on a point basis and, unless satellite density is sufficient, it is

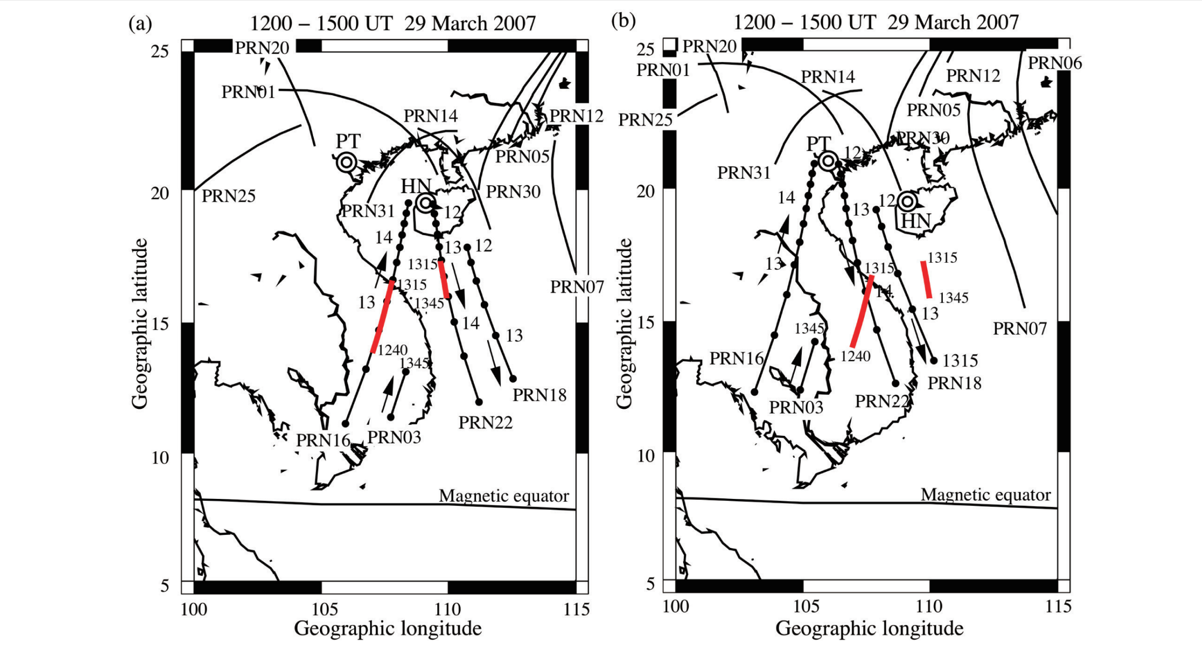

Fig.9 (a) GPS satellite's trajectory seen from Hainan, China, at 12:00 to 15:00 UT on March 29, 2007; (b) Trajectory seen from Phu Thuy, Vietnam
The black dots on the line represent satellite position every 15 minutes, while the numbers indicate the times of day (UT). The red line indicates the location where intense scintillation was observed at Hainan[9].

possible to overlook a plasma bubble.

The occurrence of scintillation over Hainan switched from PRN 18 to PRN 22, with 13:15 UT marking the borderline. The scintillation at PRN 22 then continued until 13:45 UT. From this, the relation between plasma bubbles and the trajectory of IPP of the PRN 18 and 22 satellites can be estimated as shown in Fig. 10. In the meantime, assuming that plasma bubbles move at a constant velocity without changing shape, one can estimate the actual drift velocity of plasma bubbles. As shown in Fig. 10, plasma bubbles can be assumed to travel about 270 km eastward in 30 minutes, so that the actual drift velocity of plasma bubbles is 150 m s^{-1} eastward. This velocity is very close to the drift velocity of 130 m s^{-1} for plasma irregularities estimated based on movement of the scintillation pattern. From this finding, concerning the plasma bubbles observed at a longitude near Hainan on March 29, 2007, one can say that virtually the same results were obtained for the drift velocities of plasma bubbles, plasma irregularities, and the large-scale structure of the lower ionosphere as estimated from HF-TEP.

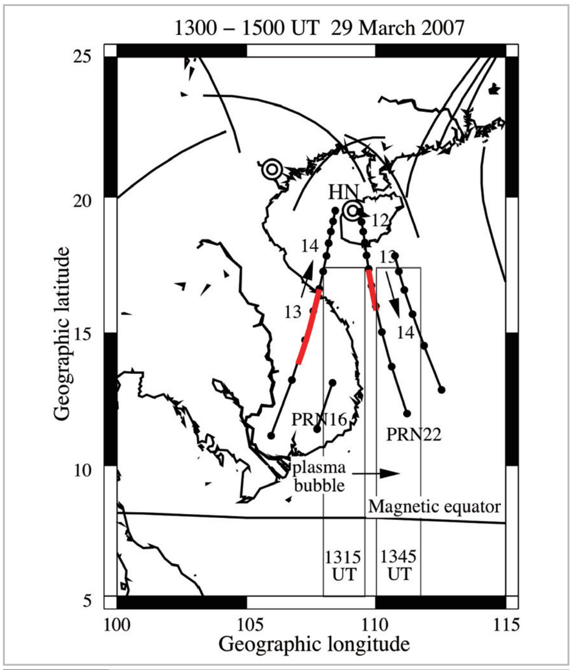

Fig.10 Similar to Fig. 9 but showing the locations of plasma bubbles estimated from 13:15 UT to 13:45 UT on March 29, 2007[9].

Table 4 compares the drift velocity of small-scale plasma irregularities estimated

Table 4 *East-west drift velocities (m s^{-1}, positive eastward) estimated in HF-TEP and GPS scintillation*

Date	Oarai (near the azimuth angle of 226º)	GPS scintillation (Hainan)
March 26, 2007	77	80
March 29, 2007	93	130
March 31, 2007	93	80
April 15, 2007	-	95
September 18, 2007	-	50
October 22, 2007	39	-

"-" indicates lack of measurement or failure to estimate velocity.

based on GPS scintillation observed at Hainan with the drift velocity of the large-scale structure of the bottom side ionosphere estimated based on HF-TEP observed at Oarai. From this comparison, one can see that these groups of velocities almost agree with each other. On September 18, 2007, the HF-TEP signals were so weak that we were unable to estimate velocity. Moreover, on October 22, 2007, the elevation angle of the GPS satellite for which scintillation was observed at Hainan was too low, also resulting in failure to estimate velocity there as well. Huba et al.[14]. conducted a study based on numerical simulation to demonstrate that the E×B drift velocity inside a plasma bubble can differ from the plasma bubble's upper development velocity. This means that the velocity of plasma does not necessarily agree with the velocity of the plasma bubble itself. The difference in velocity between small-scale plasma irregularities and the large-scale ionospheric structure obtained in this study was within the range of error in the observation method employed by this study. In this way, it is difficult to derive a clear conclusion from this study concerning the issue presented by Lin et al.[8]. regarding the difference in velocity between small-scale plasma irregularities and the large-scale ionospheric structure. Although HF-TEP and GPS scintillation were simultaneously observed during low solar activity period, resulting in few observation findings, this simultaneous observation of OGCP and scintillation produced results where the velocities estimated by using both virtually agree with each other, demonstrating that OGCP seen in HF-TEP at nighttime stemmed from plasma bubbles. Therefore, this finding marks an important discovery.

HF radio waves propagated across the equator are presumably reflected on the borders of plasma bubbles below the peak in the ionospheric F region. Scintillation intensity is proportional to the absolute value of change in ionospheric plasma density, so that plasma irregularities near the peak of the ionospheric F region are considered to affect scintillation most intensely. In fact, in observations made at Hainan on March 29, 2007 (Fig. 10), the drift velocity in the scintillation region almost agreed with the drift velocity of plasma irregularities. From these findings, both methods (HF-TEP and GPS scintillation) were presumably sensitive in the same altitude region of the ionosphere, since the two methods yielded very similar values in estimated velocities.

5 Conclusion

This study presented the results of simultaneously observing HF-TEP and GPS scintillation for the first time in the world. HF-TEP was observed by measuring the arrival angle of Radio Australia's broadcast waves transmitted from Shepparton, Australia, by using the direction exploratory equipment in Oarai, Japan. GPS scintillation was observed at Hainan, China, and at Phu Thuy, Vietnam. Observations at Phu Thuy obtained little data due to the poor condition of the equipment there, but GPS scintillation generated over Hainan agreed well with HF-TEP OGCP generated near a azimuth angle of 226° in Oarai. Moreover, the drift velocity of small-scale (300−400 m) plasma irregularities stemming from plasma bubbles estimated based on movement of the GPS scintillation pattern on the ground agreed well with the drift velocity of the large-scale structure of the bottom side ionosphere, as estimated based on changes in the arrival angle of HF-TEP. These findings proved that nighttime OGCP seen in HF-TEP is associated with plasma bubbles, and that HF-TEP is quite effective in the wide-range monitoring of plasma bubbles. The arrival angle of OGCP in HF-TEP is obscure and leaves errors in estimating location and velocity. For monitoring the generation and movement of plasma bubbles, it is very important to more precisely estimate the location and velocity of plasma bubbles. The scattered arrival angle is presumably due to the fact that HF broadcast waves take several different propagation paths; therefore, it is more effective to measure the propagation path length, thereby distinguishing the propagation paths. An effective method of measuring propagation path length is passive radar whereby reception is observed simultaneously at two locations (near the radio source and at a remote location) and propagation time is determined based on the resulting lags in waveform. As of 2009, with the grant-in-aid for young scientists (B) provided by the Ministry of Education, Culture, Sports, Science and Technology of Japan (MEXT), a system for wide-range monitoring of the generation and movement of plasma bubbles by using passive radar is being developed. In the future, TEP observations with VHF radio waves that travel more straightly should be conducted with a specially prepared transmitter.

Large safety margins to cover the possibility of overlooking the presence of plasma bubbles have been considered for the MTSAT satellite-based augmentation system (MSAS), ground-based augmentation system (GBAS), and other advanced uses of satellite navigation. Such an approach would pose an obstacle to more advanced use of such technologies. However, when it becomes possible to unfailingly monitor plasma bubbles and predict their movement, it will also become possible to reduce unnecessary safety margins, thereby paving the way to more advanced use of satellite navigation. Monitoring the generation and movement of plasma bubbles by observing the OGCP of HF-TEP is a promising method that will enable the more advanced use of satellite navigation, which must be actively promoted not only for scientific purposes but also for social benefit.

Acknowledgments

Observations at Hainan and Phu Thuy were made according to the research agreements established between the National Institute of Information and Communications Technology (Japan), the Chinese Academy of Sciences, and the Vietnam Academy of Science and Technology, respectively. The authors wish to thank Dr. Ma and Ms. Li of the National Astronomical Observatories, Chinese Academy of Sciences, Ms. Chen of the Center for Space Science and Applied Research, Chinese Academy of Sciences, and Dr. Ha Duyen and Mr. Le Truong of the Vietnam Academy of Science and Technology. The authors also wish to thank Mr. Masabumi Kawamura for acquiring data with the Oarai direction finder, as well as all members of the SEALION Project.

References

1 Röttger, J., "Wave-like structures of large-scale equatorial spread-F irregularities," J. Atmos. Terr. Phys., Vol. 35, pp. 1195–1206, 1973.

2 Maruyama, T. and M. Kawamura, "Equatorial ionospheric disturbance observed through a transequatorial HF propagation experiment," Ann. Geophys., Vol. 24, pp. 1401–1409, 2006.

3 Valladares, C. E., R. Sheehan, S. Basu, H. Kuenzler, and J. Espinoza, "The multi-instrumented studies of equatorial thermosphere aeronomy scintillation system: Climatology of zonal drifts," J. Geophys. Res., Vol. 101, pp. 26839–26850, 1996.

4 Kil, H., P. M. Kintner, E. R. de Paula, and I. J. Kantor, "Global Positioning System measurements of the ionospheric zonal apparent velocity at Cachoeira Paulista in Brazil," J. Geophys. Res., Vol. 105, pp. 5317–5327, 2000.

5 Kintner, P. M., B. M. Ledvina, E. R. de Paula, and I. J. Kantor, "The size, shape, orientation, speed, and duration of GPS equatorial anomaly scintillations," Radio Sci., Vol. 39, pp. RS2012, doi: 10.1029/2003RS002878, 2004.

6 Ledvina, B. M., P. M. Kintner, and E. R. de Paula, "Understanding spaced-receiver zonal velocity estimation," J. Geophys. Res., Vol. 109, pp. A10306, doi: 10.1029/2004JA010489, 2004.

7 Otsuka, Y., K. Shiokawa, and T. Ogawa, "Equatorial ionospheric scintillations and zonal irregularity drifts observed with closely-spaced GPS receivers in Indonesia," J. Meteor. Soc. Japan, Vol. 84A, pp. 343–351, 2006.

8 Lin, C. S., T. J. Immel, H. -C. Yeh, S. B. Mende, and J. L. Burch, "Simultaneous observations of equatorial plasma depletion by IMAGE and ROCSAT-1 satellites," J. Geophys. Res., Vol. 110, pp. A06304, doi: 10.1029/2004JA010774, 2005.

9 Saito, S., T. Maruyama, M. Ishii, M. Kubota, G. Ma, Y. Chen, J. Li, C. Ha Duyen, and T. Le Thurong, "Observations of small- to large-scale ionospheric irregularities associated with plasma bubbles with a transequatorial HF propagation experiment and spaced GPS receivers," J. Geophys. Res., Vol. 113, A12313, doi: 10.1029/2008JA013149, 2008.

10 Kelley, M. C., J. J. Makela, L. J. Paxton, F. Kamalabadi, J. M. Comberiate, and H. Kil, "The first coordinated ground- and space-based optical observations of equatorial plasma bubbles," Geophys. Res. Lett., 30, Vol. 1766, 10. 1029/2003GL017301, 2003.

11 Keskinen, M. J., S. L. Ossakow, and B. G. Fejer, "Three-dimensional nonlinear evolution of equatorial spread-F bubbles," Geophys. Res. Lett., Vol. 30, pp. 1855, doi: 1029/2003GL017418, 2003.

12 Briggs, B. H., G. J. Philips, and D. H. Shinn, "The analysis of observations on spaced receivers of the fading of radio signals," Proc. Phys. Soc. Sec. B, Vol. 63, pp. 106–121, 1950.

13 Fejer, B. G., E. R. de Paula, S. A. Gonzaréz, and R. F. Woodman, "Average vertical and zonal F region plasma drifts over Jicamarca," J. Geophys. Res., Vol. 96, pp. 13901–13908, 1991.

14 Huba, J. D., G. Joyce, and J. Krall, "Three-dimensional equatorial spread F modelling," Geophys. Res. Lett., Vol. 35, pp. L10102, 10.1029/2008GL033509, 2008.

***SAITO Susumu**, Ph.D.*

Senior Researcher, Communication, Navigation, and Surveillance Department, Electronic Navigation Research Institute

Aeronomy, Satellite Navigation

***MARUYAMA Takashi**, Ph.D. (Eng.)*

Executive Researcher

Upper Atmospheric Physics

***ISHII Mamoru**, Dr. Sci.*

Director, Project Promotion Office, Applied Electromagnetic Research Center

Upper Atmospheric Physics

***KUBOTA Minoru**, Ph.D.*

Senior Researcher, Space Environment Group, Applied Electromagnetic Research Center

Aeronomy